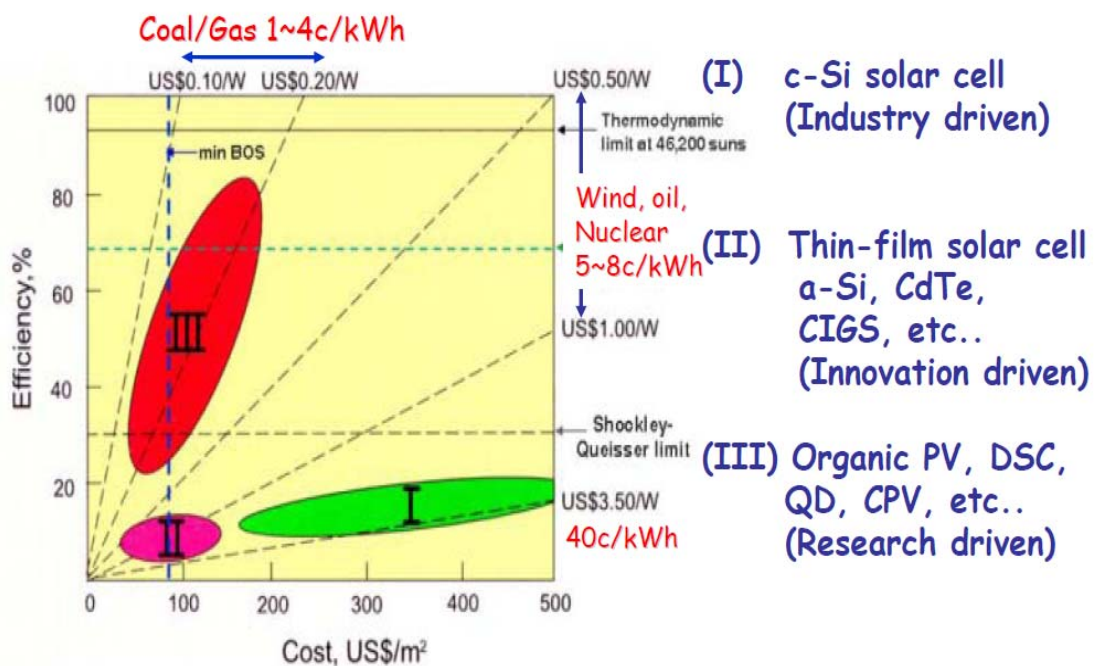


Organic Solar Cells

有機太陽能電池

近年來的發展與應用



PLASTIC SOLAR CELLS EMPLOYING ELECTRODEPOSITED ZNO AND ORGANIC PHOTOSENSITIZER DYES

Tsukasa Yoshida¹, Masaki Matsui², Kazumasa Funabiki¹, Hidetoshi Miura² and Yoshiya Fujishita³
¹ Center of Innovative Photovoltaic Systems (CIPS), Gifu University, Japan, ² Chemieca Inc., Japan, ³ Sekisui Jushi Corp., Japan

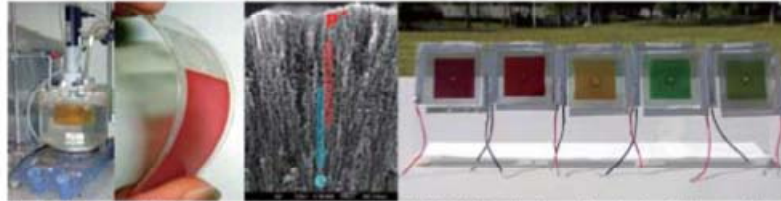


Fig. 1 Electrodeposition bath employing RDE, ZnO/eosinY hybrid thin film electrodeposited on ITO coated PET film, nanowire porous structure of electrodeposited ZnO thin film (cross section SEM) and colorful plastic solar cells (from left to right).

$\eta = 5.6\%$
for small cell

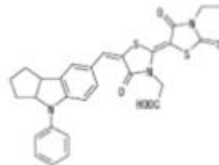


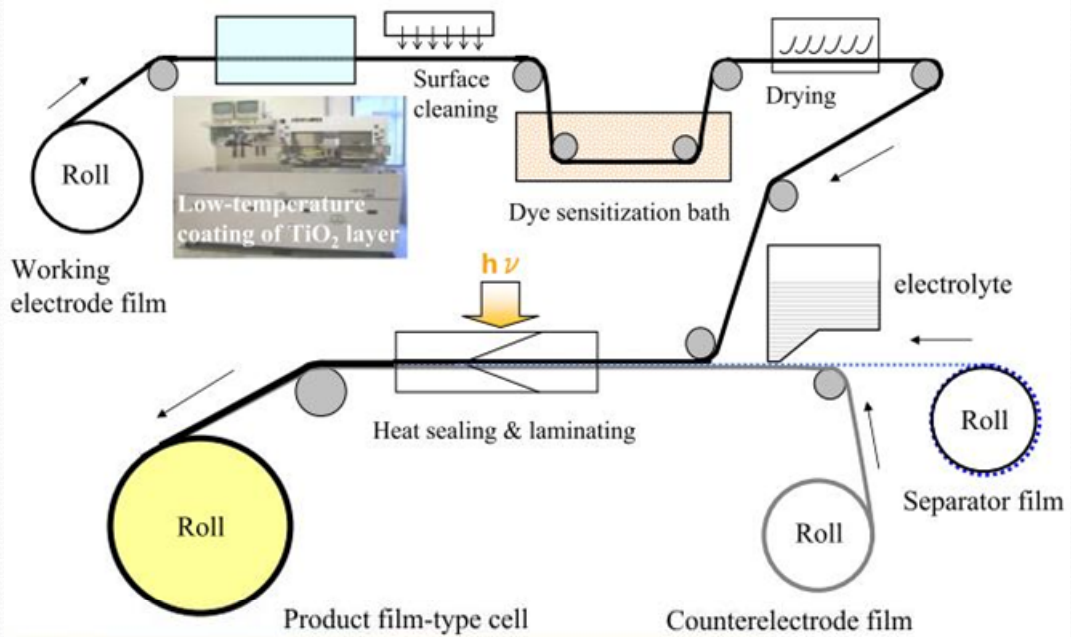
Fig. 2 The structure of new DN-7 dye.



Fig. 3 Full plastic submodule (10 cm × 10 cm) with promising 3.2% conversion efficiency (active area) employing electrodeposited ZnO and organic photosensitizer dye.

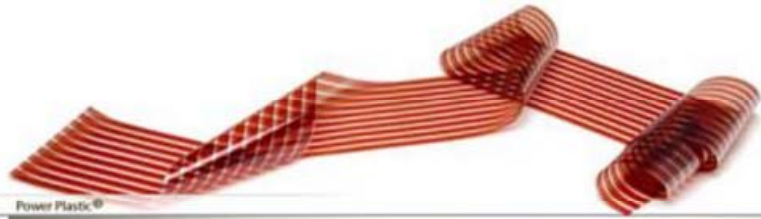
Technical Digest of the International PVSEC-17, Fukuoka, Japan, 2007

Roll-to-Roll Manufacturing Process





Konarka — Power Plastic



染料敏化太陽電池 vs 矽基太陽電池

- 製程容易、成本低
- 轉換效率隨溫度上成而提升
- 模板二面皆可吸收光線-有利於吸收散射光
- 轉換率對入射光角度影響較小
- 具有的透明性可直接使用於窗戶- 模板顏色因使用的染料顏色而變
- 能源回收期(數月)遠小於矽晶太陽電池(數年)

Source from Prof. M. Grätzel



單晶矽



多晶矽



非晶矽



多色系染料
太陽電池板



可撓式染料
太陽電池



Roll-to roll
製程染料太
陽電池



Battery charger



G24 Innovations, UK

Graetzel-type
"Roll to Roll" process
Plastic Modules



The skylight of a car



The 39th Tokyo Motor Show 2005 MAZDA STAND INFORMATION

Concept model "SENKU" (先驅)

Glass roof equipped with DSC



DSC

Nothing was revealed about the solar cell.





Features of DSSC



CEATEC JAPAN -- TDK



Ref: Prof. Yoshida's Lecture

PV EXPO 2008 — Peccell



Ref: Prof. Yoshida's Lecture

Power Dressing

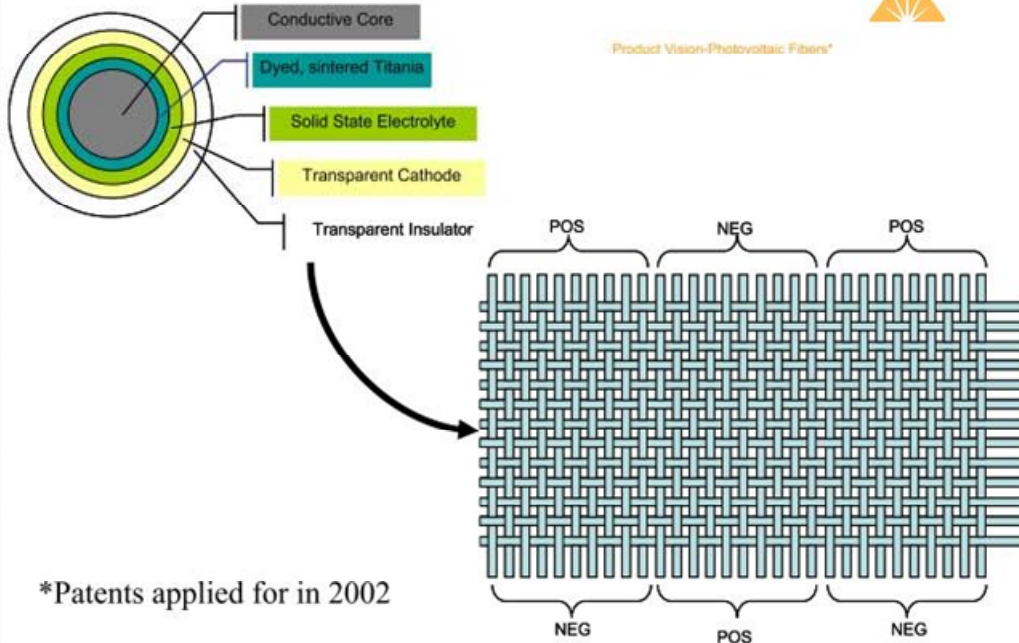


Ref: <http://apchem.gifu.u.ac.jp/~pcl/special/frame1.htm>



National Taiwan University

Photovoltaic Fibers (Konarka)



Consumer Electronics

Powering a camera in the rain forest (Bresil)



(5W)

Enabling battery charge wherever you go!



Get up to 100% charge for your electronic devices (not included)

flexcell
flexible PV technologies

Emergency

Hurricane Disaster in New Orleans 2005



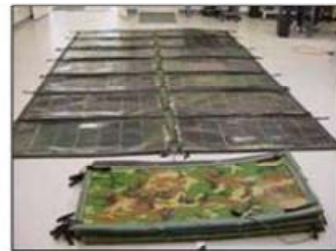
Powerless. Downed wires were a common sight in the hurricane disaster zone. Over one million citizens had no access to electricity, and for more than 100,000 the situation won't change for some time.



On line, Bill Ball (left) poses with port technician «Buddy» in front of his 2.4 kW mobile PV system, here powering equipment at a New Orleans port's temporary offices.



With PV back up systems, operations of crucial infrastructure could have been continued in flooded New Orleans. But the Gulf Coast states hit by Katrina offer hardly incentives.



Source : Photon International, November 2005

Military



TIPV (Textile Intergrated Photovoltaics)



Moto Solar Urbana



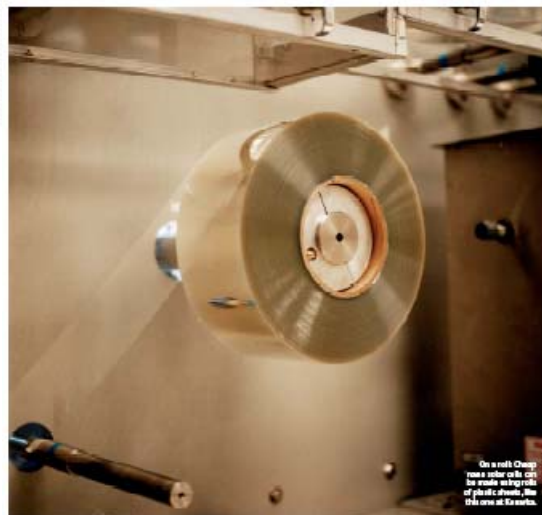
2007巴塞隆納車展 — 最佳創意科技大獎

<http://sun-red.com/>



臺灣大學 National Taiwan University

Handheld power: Konarka's solar film is light and flexible and could be laminated onto portable devices.



On a roll: Cheap nano solar cells can be made using rolls of plastic sheets, like this one at Konarka.



Conclusion: Efficiency vs. Lifetime

	2008	2010	2012	2014+
Applications	<ul style="list-style-type: none">• Consumer• Military• Indoor	<ul style="list-style-type: none">• Consumer• Military• Awning• Indoor	<ul style="list-style-type: none">• Consumer• Military• Indoor• Stationary• Architectural	<ul style="list-style-type: none">• Architectural• Consumer• Military• Indoor• Stationary
Key Features				
• Lifetime	3y	3-5y	10y	15y
• Efficiency	3%	5%	7.5%	10+%
• Price	> \$7.00/W	\$5/Wp	\$2.60/Wp	\$1.00/Wp
• Weight	60 mW/g	50 mW/g	30 mW/g	30 mW/g
Market Size	\$25 M	\$250 M	\$1.5 B	\$10 B
Volume	3.5 MW	50 MW	500 MW	10,000 MW



Cite this: *Soft Matter*, 2012, **8**, 1467

www.rsc.org/softmatter

PAPER

Self-assembled multilayers of modified ITO in polymer solar cells by soft-imprinting

Li-Chen Huang,^{ab} Hung-Wei Liu,^c Chin-Wei Liang,^c Tsu-Ruey Chou,^{ab} Leeyih Wang^{*cd} and Chih-Yu Chao^{*ab}

Received 27th September 2011, Accepted 7th November 2011

DOI: 10.1039/c1sm06837g

Optimized performances of polymer solar cells has been of magnificent interest in recent years. A variety of approaches have been reported to alter or replace the polymer buffer layers in solar device structures. In this present work, surface modification of indium tin oxide (ITO)-coated substrates through the use of self-assembled multilayers by the soft-imprinting method has been applied to adjust the anode work function and device performance in polymer solar cells based on a P3HT:PCBM heterojunction. The efficiency and morphology of the solar device with CF₃-terminal group materials as a buffer layer have been measured and investigated. These results demonstrate that the soft-imprinting method is an effective and rapid procedure that enhances the quality of polymer solar cells and indicates potential implications for other organic devices containing an interface between a blended organic active layer and an electrode layer.

1. Introduction

Organic photovoltaic (OPV) cells hold great promise for clean energy generation by converting sunlight into electricity since solar power is an abundant energy source and can be used anywhere.¹ In particular, it provides relatively inexpensive materials and simple solution processable substitutes to inorganic-based photovoltaic devices.² In addition, the advantages of using solar cell devices made from organic systems are that they possess mechanical flexibility, are light weight, and can be produced using roll-to-roll manufacturing methods at low temperatures. One of the most representative OPV cells is the device based on a blend of poly(3-hexylthiophene) (P3HT) as an electron donor and a soluble C₆₀ derivative, [6,6]-phenyl-C₆₁-butyric acid methyl ester (PCBM) as an electron acceptor. Although the conversion efficiency of the conventional bulk-heterojunction (BHJ) solar cell architecture consisting of P3HT:PCBM has reached over 4–6% by a variety of processes,³ its performance is still restrained by a relatively poor carrier transfer property, which has also impeded the path towards commercialization. Good photovoltaic devices require the optimization of phase separation and morphology formation in a blended film and also the development of new materials to allow improved

interfacial contact in a balanced hole and electron charge transport. Generally, the efficiency of organic devices can be enhanced significantly when a poly(3,4-ethylenedioxythiophene):poly(styrenesulfonate) (PEDOT:PSS) layer is introduced to facilitate hole transport/injection in light-emitting diodes⁴ or as a buffer layer in solar cells.⁵ Nevertheless, it is well known that the indium tin oxide (ITO) glass is very sensitive to acidic environments. Due to the strong acidic nature of PSS, the aqueous solution from which the PEDOT:PSS films are cast can also be expected to etch the ITO.⁶ Also, this polymer buffer layer in the organic electronic device structure can be easily oxidized in air, which leads to a deterioration in performance.

To date, many approaches, such as oxygen-plasma etching, UV-ozone treatments,⁷ and self-assembling of monolayers of dipolar molecules,⁸ have been delicately tailored to improve the properties of ITO substrates. Self-assembled monolayer (SAM) modification, one of the most promising methods, has been employed to alleviate this problem. It is used to insert a less air-sensitive buffer layer between the active layer and electrode in order to reduce the amount of degradation and the amount of oxygen and moisture diffusion inside the organic active layer.⁹ Self-assembled monolayers of organic compounds on inorganic or metal surfaces are becoming increasingly important in many areas of material science.¹⁰ Moreover, some research groups utilized self-organized layers as buffer layers to control the surface energy of the materials¹¹ and to alter the work function of the charge collecting electrodes in molecular solar cells.¹² However, the regular immersion method is incapable of producing various patterns that are designed.¹³ A new strategy is desirable for the mass production of layer structures on a wide variety of substrates, which can be applicable to various fields of manufacturing, for example, microelectronics, micro-optics, and

^aDepartment of Physics, National Taiwan University, Taipei, 10617, Taiwan. E-mail: cychao@ntu.edu.tw; Fax: +886-2-33665088; Tel: +886-2-33665130

^bInstitute of Applied Physics, National Taiwan University, Taipei, 10617, Taiwan

^cInstitute of Polymer Science and Engineering, National Taiwan University, Taipei, 10617, Taiwan

^dCenter for Condensed Matter Sciences, National Taiwan University, Taipei, 10617, Taiwan. E-mail: leewang@ntu.edu.tw; Fax: +886-2-23655404; Tel: + 886-2-33665276

organic photovoltaics. The soft-imprinting method is one very important technique to fulfil this requirement since this system provides suitable and fast experimental simplicity and flexibility for some complex work, such as organic photovoltaic devices. Furthermore, the soft-imprinting method offers a remarkable ability to form as many diverse patterns as possible.¹⁴

In this paper, we employed self-assembled multilayers with terminal $-\text{CF}_3$ groups to modify the surface characteristics of ITO substrates by the soft-imprinting method, and investigated the effects of these treatments on the morphology of the active layer, the work function of the ITO electrode and the resultant OPV performance. In BHJ solar cells using P3HT:PCBM, adjustment of surface energy and work function of ITO may lead to a tuneable morphology for the active layer and hole injection barrier reduction. As-modified ITO substrates were characterized with contact angle measurements, ultraviolet photoemission spectroscopy, UV-vis optical measurements and atomic force microscope imaging. The obtained results show that the work function of the modified ITO substrates is close to the highest occupied molecular orbital level (HOMO) of P3HT, and thus helps to reduce the barrier of hole injection. By means of CF_3 -material modification, the device performances including the short-circuit current density (J_{sc}) and fill factor (F.F.) are enhanced. As a result, the CF_3 -material treated sample has improved the efficiency of hole injection into the ITO and exhibited a higher power conversion efficiency, which is comparable to that of the device with a PEDOT:PSS insertion layer. Moreover, we found the soft-imprinting method which can be applied to adjust the anode work function is an efficient and fast approach for large scale flexible polymer solar cells.

2. Experimental section

A schematic diagram of the soft-imprinting method for fabricating self-assembled multilayers is illustrated in Fig. 1, and can be mainly described by the following steps. First of all, this process uses a stamp to print self-assembled multilayers onto the ITO glass in order to modify the surface properties of the ITO substrate. The soft stamp, poly(dimethylsiloxane) (PDMS), plays a crucial role in standard microcontact printing (μCP) techniques and can easily make conformal contact with different surfaces. In Fig. 1(a), wetting of the elastomeric stamp was accomplished by exposing the stamp to a 0.5 wt% solution of trimethoxy(3,3,3-trifluoropropyl)silane (CF_3 -silane for short) in hexane, either by pouring the solution over the surface of the stamp or by rubbing the stamp moderately with a Q-tip which has been saturated with the CF_3 -silane solution. Hydroxyl groups were introduced to the ITO substrate by carrying out O_2 -plasma treatment for 15 min previously. Following the wetting step, the stamp was slowly brought into contact with the surface of ITO glass substrate in an ambient environment, as shown in Fig. 1(b). Typically, very light pressure is applied by hand in order to help complete the contact between the stamp and the surface, and to squeeze out any air bubbles. Then, the stamp was gently peeled off from the surface, as seen in Fig. 1(c). After the removal of the stamp, the CF_3 -silane materials were transferred from the stamp to the ITO upon contact, and covalently bonded to the underlying ITO surface.¹⁵ Then, the substrate was rinsed with hexane to remove the residual molecules. Eventually, the ITO substrate was sheerly

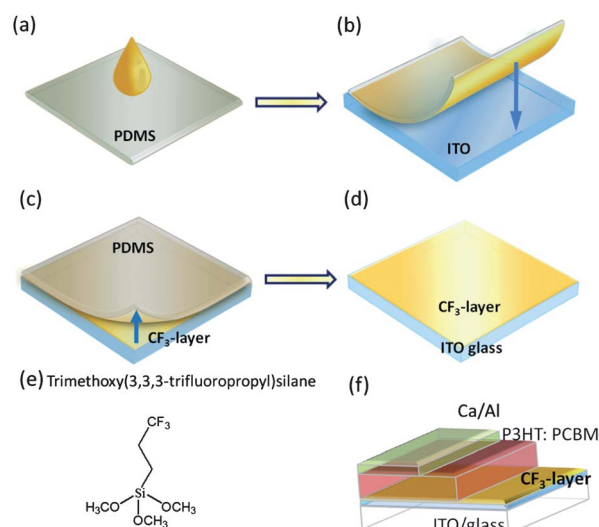


Fig. 1 Schematic representation of the formation of self-assembled multilayers by the soft-imprinting method. (a) The CF_3 -silane solution was deposited on the surface of the PDMS film. (b) The CF_3 -silane-coated PDMS film was inversely attached onto the ITO surface. (c) The top transparent PDMS film is peeled off from the ITO substrate. (d) After the removal of the stamp, the self-assembled multilayers of CF_3 were formed onto the ITO surface. (e) Chemical structure of the CF_3 -silane material. (f) The polymer solar cell device structure consisting of ITO/ CF_3 -layer/P3HT:PCBM/Ca/Al.

modified with CF_3 -silane materials, as shown in Fig. 1(d). Also, the procedure can be conducted under atmospheric pressure in an unprotected laboratory environment. The chemical structure of the CF_3 -silane material is shown in Fig. 1(e). Furthermore, CF_3 -silane materials exhibit many positive characteristics: ease of preparation, good stability under ambient conditions, relatively low densities of defects in the final structures, and amenability to applications in controlling interfacial properties. Herein, CF_3 -layers with electron-withdrawing groups can increase the work function of the ITO/active layer interface and causes the hole injection barrier of ITO to become closer to the highest occupied molecular orbital level (HOMO) of the active layer. In many such applications, the work function of ITO has a profound effect on device performance because it affects the energy barrier height at the heterojunction interface. Subsequently, the CF_3 -layer treated ITO was coated with a P3HT:PCBM blend in 1,2-dichlorobenzene (ODCB) to analyze the electrical properties of the modified ITO surfaces. Finally, a cathode comprised of stacked Ca (20 nm) and Al (100 nm) layers was evaporated onto the surface of the active layer to achieve a polymer solar cell. The complete device structure of a polymer solar cell is illustrated in Fig. 1(f).

An elastomeric stamp applied to the ITO surface is the key to the soft-imprinting method. In addition to its elasticity, the PDMS elastomer has many other benefits that make it extremely useful in the soft-imprinting process: (a) the PDMS has good chemical stability and makes conformal contact with rigid surfaces over relatively large areas. (b) The PDMS is not hydroscopic; it does not swell with humidity. (c) The PDMS elastomer has good thermal stability; prepolymers being easily molded can be cured thermally. (d) The elastomeric PDMS is

durable when it is used as a stamp; we can use a PDMS stamp many times over a period of several months without observing any degradation in performance. Therefore, we chose to use the elastomeric PDMS polymer for our soft-imprinting experiments.

The PDMS stamps were prepared by cast molding: a mixture of Sylgard 184 silicon elastomer (Dow Corning) and a curing agent (10 : 1 ratio by volume). The raw material is supplied as a two-part kit: a liquid silicon rubber base (*i.e.* a vinyl-terminated PDMS) and a curing agent (*i.e.* dimethylsiloxane).¹⁶ The two compounds were stirred in a vessel for 20 min and degassed in a centrifuge for 5 min before it was mildly poured onto the flat substrate to be solidified. In order to make a smooth surface stamp, the liquid mixture was poured onto a silicon wafer which was formerly deposited with an anti-stick solution and then it was cured at 70 °C in an oven for 4 h. The anti-stick solution is (tridecafluoro-1,1,2,2-tetrahydrooctyl)dimethylchlorosilane (FOTS) which is purchased from the Gelest company. The PDMS stamps were peeled away from the FOTS-coated silicon wafer after cooling and placed on a glass surface, they were then cut into pieces (1 cm × 1 cm). The thickness of the PDMS was around 2 to 4 mm.

For the sake of the soft-imprinting procedure, the PDMS stamps wetted with the CF₃-silane solution were usually lifted with tweezers, and softly attached to the ITO substrate to transfer the CF₃-silane materials. The 0.5 wt% CF₃-silane (Aldrich) solution was completely dissolved in a hexane solution. The ITO was first cleaned by scrubbing in a detergent, then thoroughly rinsed in deionized water, and finally sonicated in acetone and IPA. The ITO glass substrate was treated with O₂-plasma before the coating of the buffer layers in order to improve the adhesion between the ITO surface and the CF₃-silane film. For comparison, the CF₃-silane film was also replaced by PEDOT:PSS in our system as a control sample. The thickness of the CF₃-silane layer is ~6 nm which was characterized by a spectroscopic ellipsometer (J. A. Woollam VASE).

Polymer solar cells were fabricated *via* a combination of spin-coating and the soft-imprinting method on ITO glass substrates (2 cm × 2 cm). For comparison with the device using CF₃-silane treated ITO, a commonly used PEDOT:PSS (Baytron P VP AI4083) was spin-coated (40 nm) on the ITO glass, followed by heating at 140 °C for 10 min. The mixtures of P3HT (15 mg ml⁻¹) and PCBM (Nano-C, 12 mg ml⁻¹) were soluble in 1,2-dichlorobenzene (ODCB). Meanwhile, those substrates were delivered into a nitrogen-filled glove box and the P3HT:PCBM layer was later spin-coated on top of the PEDOT:PSS pre-coated ITO substrate (15 Ω □⁻¹). The thickness of the active layer was *ca.* 200 nm and the device area was 0.06 cm², which was defined by a shadow mask. Metallic cathodes of Ca (20 nm) and Al (100 nm) were successively evaporated on it under high vacuum conditions of 10⁻⁶ Torr. Thermal annealing was performed at 110 °C for 10 min under a N₂ atmosphere after the deposition of the cathode. To study the performances of solar cells applying these modified ITO substrates, the current density–voltage (*J*–*V*) characteristics were measured in the dark and under AM1.5G solar illumination at an intensity of 100 mW cm⁻², which was obtained from a 300 W Xe lamp solar simulator (Oriel 91160) utilizing a programmable Keithley mode 2400 instrument. Light intensity was calibrated by a mono-Si reference with a KG5 filter (PV Measurements, Inc.),

which was calibrated by the National Renewable Energy Laboratory.

After the imprinting process, the sample for ultraviolet photoelectron spectroscopy (UPS) measurements was stored in a vacuum desiccator and exposed briefly to the air before being placed into an ultra-high-vacuum (UHV) chamber equipped with an angle-resolved electron energy analyzer. The UPS (Thermo VG-Scientific) measurements were performed using the He I photo line ($h\nu = 21.22$ eV) of a He discharge lamp under UHV conditions (2×10^{-11} Torr). When the data was collected, the samples were biased at -5 V in order to measure the onset of the photoemission spectra, which was used to determine the position of the work function of the modified ITO surface. The as-treated ITO surface was also characterized by taking multiple advanced contact angle measurements (First Ten Angstrom) from various locations on the substrate, which was modified with or without the CF₃-silane materials. The absorption and transmission spectra of the active layer and CF₃-silane thin film were visualized with the aid of a UV-vis spectrometer (JASCO). The morphology of the active layer surface coated on the top of the PEDOT:PSS and CF₃-silane-coated ITO was investigated under the atomic force microscope (PSIA XE-100).

3. Results and discussions

3.1 Electrode work function and surface wettability

Examples of He I UPS spectra of modified ITO substrates are revealed in Fig. 2, where the first derivative of the secondary-cutoff region of the UPS spectrum is shown in Fig. 2(b). The spectrum in Fig. 2(a) was taken for a sample with a -5 V bias so that the sample inelastic cutoff could be distinguished from the spectrometer. This cutoff, also called the photoemission onset, is related to the vacuum level (E_{vac}) because no electrons with less

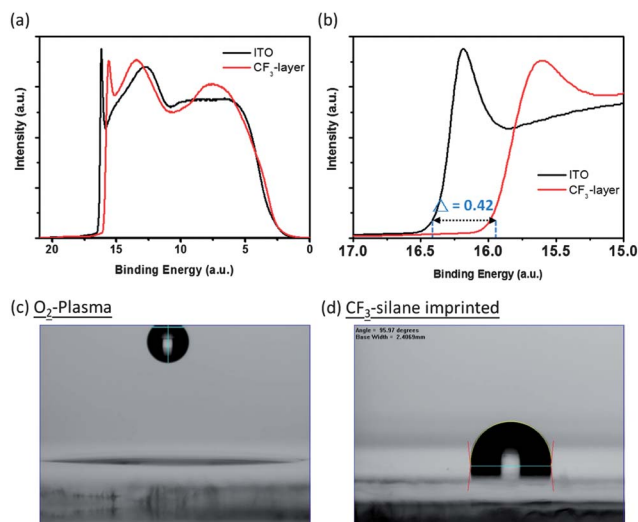


Fig. 2 (a) UPS spectra of the bare ITO and CF₃-silane modified ITO surfaces. (b) Close-up of the secondary electron edge (15–17 eV). Shift in binding energy is indicated as the dotted line, which is 0.42 eV. (c) The contact angle ($\sim 0^\circ$) of the O₂-plasma treated ITO substrate. (d) The contact angle of the CF₃-silane modified ITO substrate by the soft-imprinting method is 96° .

energy can escape from the solid surface.¹⁷ The onset of photoemission corresponds to the changes in the work function at the ITO surface. The main cutoff of the secondary electron edge was used to determine the work function after each preparation step. Therefore, the work function can be calculated by subtracting the binding energy of the secondary electron edge from the He I excitation energy (21.22 eV).¹⁸ As a result, through the addition of the CF₃-layer to the ITO glass substrate, a work function shift was observed. The work function of the ITO substrate in our experiment is 4.7 eV, after the O₂-plasma process. In the case of the CF₃-terminated layer, the onset of secondary electrons is 0.42 eV higher than that of the plasma treated ITO. The CF₃-layer being deposited through the soft-imprinting method, obtained a work function which is increased by 0.42 eV, to a value of 5.12 eV, which is close to the HOMO level of the active layer (~5.2 eV), and thus the hole injection barrier from the active layer to the anode is reduced. The onset of secondary electrons was determined by extrapolating two solid lines from the background and the straight onset in each spectrum. The absolute error in the determination of cut-off is estimated to be ±100 meV, while the error of spectra recorded here, relative to each other, is estimated to be smaller (about ±50 meV).

Surface modification with the CF₃-silane materials can also change the wettability of the substrate surface by replacing -OH terminal groups with fluorocarbon molecular units. Changes in wettability can affect the way it is subsequently coated with organic layers. Improved wettability results can be confirmed by measuring the static contact angle of water on treated substrates. Table 1 presents the average contact angles with ±3° uncertainty on the different ITO surfaces. The bare ITO substrate has a low water contact angle of 35°, whereas angles of nearly 0° were measured from the O₂-plasma treated ITO, as seen in Fig. 2(c). The CF₃-silane imprinted sample shows a contact angle of 96° in Fig. 2(d). An obvious increase in contact angle after the modification of ITO with the CF₃-silane materials, which primarily comes from the highly hydrophobic nature of the -CF₃ moieties, which indicates the existence of CF₃-silane on the ITO surface.

3.2 Device current–voltage characteristics

One of the critical issues concerning the high-efficiency of OPV cells, is to decrease the contact resistances of the anode and the cathode. For example, an ultrathin insulating interlayer, such as LiF, is commonly inserted between the organic active layer and the Al cathode to enhance the efficiency of electron collection.¹⁹ In order to investigate the electrical properties of the CF₃-silane treated ITO surface, an organic solar cell composed of ITO/CF₃-layer/P3HT:PCBM blend (1 : 0.8)/Ca/Al was fabricated. The ITO substrates were modified with a layer of CF₃-silane by the soft-imprinting method. For the control device, aqueous

Table 1 Static contact angle measured for ITO anodes treated in a variety of processes

Anode	Contact angle [°]
Untreated	35
O ₂ plasma	~0
CF ₃ -silane imprinted	96

dispersions of PEDOT:PSS after passing through a 0.45 μm PVDF filter were spun at 3500 rpm for 30 s on top of clean ITO substrates. The subsequent active layer was prepared the same way as the sample with a CF₃-silane buffer layer. All electrical measurements and active layer fabrications were conducted inside a glove box in which the condition is less than 1 ppm O₂ and 1 ppm H₂O. Fig. 3 shows the illuminated current density–voltage (*J–V*) curves of the P3HT:PCBM material devices fabricated on ITO (w/o buffer layer), PEDOT:PSS-coated ITO and CF₃-silane modified substrates.

Without the aid of the inserted buffer layers, such as PEDOT:PSS or CF₃-silane, the device performance shows poor results compared with the devices with buffer layers. On the other hand, the series resistance (*R_s*) of different buffer layers at a given voltage (*c.a.* 1 V) decreases from 8.4 Ω cm² (PEDOT:PSS) to 3.4 Ω cm² (CF₃-silane), which emphasized that the interfacial formation is enhanced in the CF₃-layer devices. The corresponding power conversion efficiency (PCE) increases from 3.18 ± 0.16% (PEDOT:PSS) to 3.42 ± 0.27% (imprinted). The performance parameters of all samples are summarized in Table 2. As expected, the F.F. value increases from 60.4 ± 0.5 for the PEDOT:PSS-coated device to 63.4 ± 0.5 for the CF₃-silane imprinted device, indicating a reduction in the effective series resistance, whilst the open-circuit voltage remains almost the same. Moreover, work function shifts have virtually no effect on the open-circuit voltage (*V_{oc}*), which is in accordance with the idea that *V_{oc}* is controlled intrinsically by the difference between the lowest unoccupied molecular orbital (LUMO) energy level of the acceptor and the HOMO energy level of the donor, and is insensitive to the electrode work functions.²⁰ As both *J_{sc}* and F.F. values increase with decreasing interfacial energy differences for the CF₃-silane modified device, this energetic behavior is very likely to be responsible for the behavior observed here. The *J–V* curves of all devices under simulated AM 1.5 illumination show *J_{sc}* and F.F. increase in the CF₃-silane imprinted sample. This again corresponds to the decreased *R_s* value. As a result, the CF₃-silane treated sample has improved the efficiency of hole injection into the ITO and exhibited a higher power conversion efficiency comparable to that of the device with a PEDOT:PSS insertion layer.

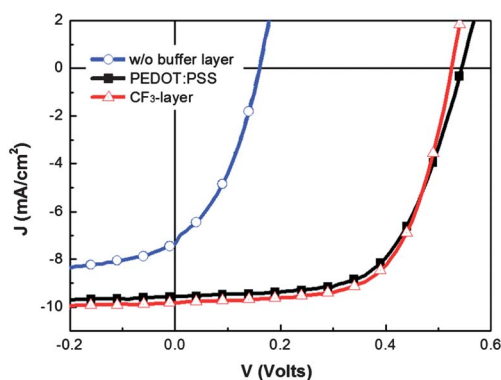


Fig. 3 *J–V* characteristics of P3HT:PCBM bulk heterojunction devices w/o a buffer layer (circle line), with PEDOT:PSS (square line) and the CF₃-layer (triangle line) under simulated AM 1.5 irradiance (100 mW cm⁻²).

Table 2 Summary of the performance parameters of the P3HT:PCBM based solar cells with and without a PEDOT:PSS layer compared with the CF₃-layer device

Buffer materials	V_{oc} (V)	J_{sc} (mA cm ⁻²)	F.F. (%)	PCE (%)
w/o	0.17	7.37	35.1	0.44
PEDOT:PSS	0.55	9.48	60.4	3.18
CF ₃ -layer	0.55	9.83	63.4	3.42

3.3 Absorption/transmission spectra and morphology of the active layer

The optical density of the P3HT:PCBM film and the transmission for the CF₃-silane modified ITO substrate are shown in Fig. 4. The transmission of the CF₃-silane treated ITO is slightly higher than that of the PEDOT:PSS layer in the range of 600 to 800 nm. Transparency is increased in the wavelength range where P3HT:PCBM absorbs, which makes this device suitable for applications which make full use of the solar illumination spectrum. The UV-vis spectrum is clearly illustrated in Fig. 4(b). Compared to the PEDOT:PSS-coated ITO glass, the CF₃-silane treated samples exhibit better light transmission characteristics in the visible light spectrum and can efficiently reduce the loss of light passing through the solar device. In addition to reaching relatively low optical absorption, the fluorocarbon surfaces

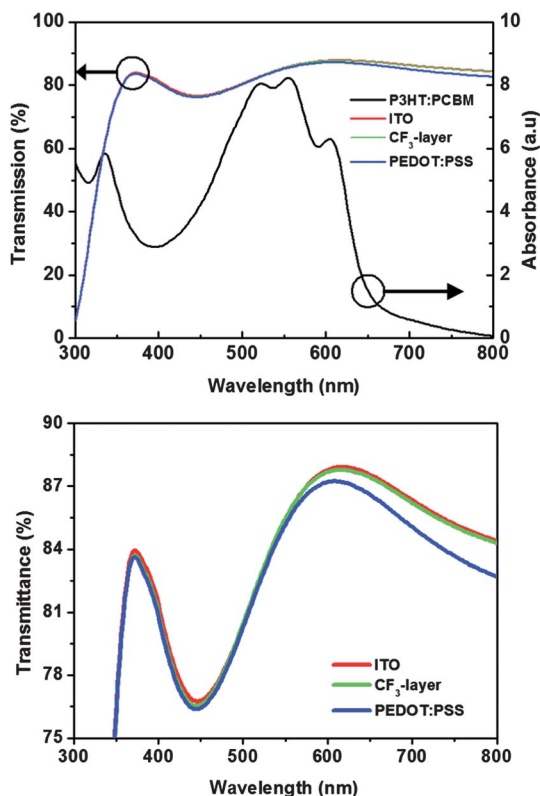


Fig. 4 Transmission of various buffer layers and absorbance of the P3HT:PCBM material in UV-vis spectra. (a) The left axis represents the transmission ratios of different buffer layers; the right axis is the UV-vis absorption spectra for the film of P3HT:PCBM (in 1 : 0.8 wt/wt ratios). (b) The transmission spectrum for the fluorocarbon layer between 610 and 800 nm is larger than that of the PEDOT:PSS-coated surface.

exhibit quite high transparency values throughout the visible light range, which is important for the application of a transparent electrode material.

In order to further validate the surface modified imprinting process, the phase image and topography of the subsequently coated active layer is investigated. In Fig. 5, the morphology of the active layers on the CF₃-silane treated ITO substrates shows a more uniform distribution of P3HT and PCBM than on the PEDOT:PSS surface after annealing. As can be seen in Fig. 5(a) and (b), the CF₃-silane treated surface could provide optimized phase separation of the P3HT:PCBM blend film due to the hydrophobic surface of the CF₃ film. The dark region refers to PCBM-rich areas; the bright area indicates the P3HT materials. As a result, the surface roughness of each sample is 4.57 nm (PEDOT:PSS/ITO) and 3.62 nm (CF₃-silane treated ITO), respectively, as shown in Fig. 5(c) and (d). The lower surface roughness indicates an increase in the number of interfaces between the donor and the acceptor. The increased interfaces are beneficial to the exciton charge separation and charge transportation which mostly contributes to the J_{sc} . The rough surface is a signature of P3HT self-organization, which increases the ordered structure formation in the active film.² Consequently, there is no excessive phase separation observed in the CF₃-sample, which means a better device performance using CF₃-silane imprinting is plausible. Rough surface morphology of the blend film may induce poorer contact between the active layer and cathode. Therefore, the CF₃-silane treated sample has optimised the active layer morphology and was found to have better performance than that of the device with a PEDOT:PSS insertion layer. The CF₃-layer serves as a passivation of inorganic surface trap states, improving the exciton dissociation efficiency at the polymer/active interface, as well as a template to influence the overlayer BHJ distribution of phase morphology, leading to better charge selectivity and enhanced solar cell performance.²¹

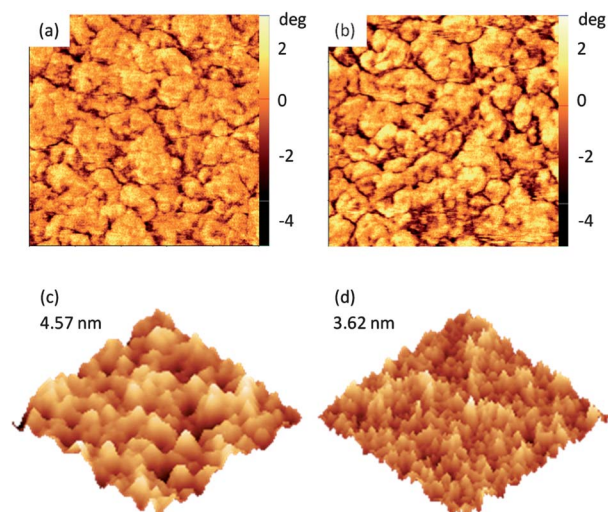


Fig. 5 Phase images of the P3HT:PCBM layer after annealing were observed under an AFM system. (a), (b): The phase images. (c), (d): The surface roughness of the active layers coated on the standard (PEDOT:PSS) and CF₃-silane treated ITO surfaces, respectively. (AFM image dimensions: 5 μ m \times 5 μ m).

4. Conclusions

The soft-imprinting method offers immediate and fast advantages in applications in which photolithography falters or fails. In summary, we have successfully proved the feasibility of the soft-imprinting method which we applied to organic solar cell devices. We note that some of these SAM-treated devices cannot easily be fabricated using existing techniques based on the conventional immersion method. In our work, the obtained power conversion efficiency (PCE) in the absence of a PEDOT:PSS layer was 3.42% for a CF₃-silane treated surface, which is higher than the corresponding PCE 3.18% of OPV cells (with PEDOT:PSS). As a result, a significant decrease in series resistance was observed in the device with a CF₃-layer. We also found that, by means of such CF₃-silane modification, both the J_{sc} and F.F. values are enhanced as compared to those of common OPV devices with PEDOT:PSS as a buffer layer. By carrying out further investigations into applications for this technique, we expect to extend this fast fabrication technique to the large scale fabrication of layer structures and to the flexible polymer solar cell industry.

Acknowledgements

The authors CYC and LW would like to thank the National Taiwan University, Academia Sinica, National Science Council, and Ministry of Education of the Republic of China for financial support on this work.

Notes and references

- 1 G. Yu, J. Gao, J. C. Hummelen, F. Wudl and A. J. Heeger, *Science*, 1995, **270**, 1789; J. Brabec, N. S. Sariciftci and J. C. Hummelen, *Adv. Funct. Mater.*, 2001, **11**, 15.
- 2 G. Li, V. Shrotriya, J. Huang, Y. Yao, T. Moriarty, K. Emery and Y. Yang, *Nat. Mater.*, 2005, **4**, 864.
- 3 W. L. Ma, C. Y. Yang, X. Gong, K. H. Lee and A. J. Heeger, *Adv. Funct. Mater.*, 2005, **15**, 1617; Y. Y. Kim, S. Cook, S. M. Tuladhar, S. A. Choulis, J. Nelson, J. R. Durrant, D. D. C. Bradley, M. Giles, I. McCulloch, C.-S. Ha and M. Ree, *Nat. Mater.*, 2006, **5**, 197; G. Zhao, Y. He and Y. Li, *Adv. Mater.*, 2010, **22**, 4355.
- 4 A. Elschner, F. Bruder, H.-W. Heuer, F. Honas, A. Karbach, S. Kirchmeyer, S. Thurm and R. Wehrmann, *Synth. Met.*, 2000, **139**, 111–112.
- 5 J. Y. Kim, K. Lee, N. E. Coates, D. Moses, T.-Q. Nguyen, M. Dante and A. J. Heeger, *Science*, 2007, **317**, 222.
- 6 M. P. de Jong, L. J. van IJzendoorn and M. J. A. de Voigt, *Appl. Phys. Lett.*, 2000, **77**, 2255.
- 7 H. K. Lee, J. K. Kim and O. O. Park, *Org. Electron.*, 2009, **10**, 1641.
- 8 Y. Vaynzof, D. Kabra, L. Zhao, P. K. H. Ho, A. T.-S. Wee and R. H. Friend, *Appl. Phys. Lett.*, 2010, **97**, 033309.
- 9 K. W. Wong, H. L. Yip, Y. Luo, K. Y. Wong, W. M. Lau, K. H. Low, H. F. Chow, Z. Q. Gao, W. L. Yeung and C. C. Chang, *Appl. Phys. Lett.*, 2002, **80**, 2788.
- 10 G. M. Whitesides, J. P. Mathias and C. T. Seto, *Science*, 1991, **254**, 1312.
- 11 Q. Wei, T. Nishizawa, K. Tajima and K. Hashimoto, *Adv. Mater.*, 2008, **20**, 2211.
- 12 S. Khodabakhsh, B. M. Sanderson, J. Nelson and T. S. Jones, *Adv. Funct. Mater.*, 2006, **16**, 95.
- 13 B. de Boer, A. Hadipour, M. M. Mandoc, T. van Woudenberg and P. W. M. Blom, *Adv. Mater.*, 2005, **17**, 621.
- 14 B. D. Gates, Q. B. Xu, M. Stewart, D. Ryan, C. G. Willson and G. M. Whitesides, *Chem. Rev.*, 2005, **105**, 1171.
- 15 D. L. Angst and G. W. Simmons, *Langmuir*, 1991, **7**, 2236.
- 16 Y. Xia and G. M. Whitesides, *Annu. Rev. Mater. Sci.*, 1998, **28**, 153.
- 17 A. Kahn, N. Koch and W. Gao, *J. Polym. Sci., Part B: Polym. Phys.*, 2003, **41**, 2529.
- 18 D. M. Alloway, M. Hormann, D. L. Smith, N. E. Gruhn, A. L. Graham, R. Colorado, V. H. Wysocki, T. R. Lee, P. A. Lee and N. R. Armstrong, *J. Phys. Chem. B*, 2003, **107**, 11690.
- 19 C. J. Brabec, S. E. Shaheen, C. Winder and N. S. Sariciftci, *Appl. Phys. Lett.*, 2002, **80**, 1288; E. Ahlswede, J. Hanisch and M. Powalla, *Appl. Phys. Lett.*, 2007, **90**, 163504.
- 20 C. J. Brabec, A. Cravino, D. Meissner, N. S. Sariciftci, T. Fromherz, M. T. Rispens, L. Sanchez and J. C. Hummelen, *Adv. Funct. Mater.*, 2001, **11**, 374.
- 21 S. K. Hau, H. L. Yip, O. Acton, N. S. Back, H. Ma and A.-Y. Jen, *J. Mater. Chem.*, 2008, **18**, 5113.

Patterning of Poly(3,4-Ethylenedioxythiophene): Poly(Styrenesulfonate) Films via the Rubbing Method in Organic Photovoltaic Cells

Li-Chen Huang¹, Hung-Wei Liu², Tsu-Ruey Chou¹, Jung Hsieh³, Wen-Yen Chiu⁴, Leeyih Wang^{2,5} and Chih-Yu Chao^{1,3}

1. Department of Physics, National Taiwan University, Taipei 10617, Taiwan

2. Institute of Polymer Science and Engineering, National Taiwan University, Taipei 10617, Taiwan

3. Institute of Applied Physics, National Taiwan University, Taipei 10617, Taiwan

4. Department of Chemical Engineering, National Taiwan University, Taipei 10617, Taiwan

5. Center for Condensed Matter Sciences, National Taiwan University, Taipei 10617, Taiwan

Received: August 02, 2014 / Accepted: August 13, 2014 / Published: August 15, 2014.

Abstract: OPV (Organic photovoltaic) cells represent a compelling candidate for renewable energy by solar energy conversion. In recent years, versatile light-trapping measures via structures have been intensively explored to optimize photovoltaic performance. In this work, a unique rubbing technique is demonstrated to create nanoscale grooves on the PEDOT:PSS [poly(3,4-ethylenedioxythiophene): poly(styrenesulfonate)] surface and the grating-like features are 500 nm wide and 10 nm deep. The PEDOT:PSS film with grooved surface is used as buffer layers for OPV cell devices based on a P3HT:PCBM bulk heterojunction. The patterned surface has a profound effect on carrier mobility, light trapping, and hole collection efficiency, leading to an increase in the short circuit density, filling factor, and power conversion efficiency. These results indicate the feasibility of the rubbing method can be applicable to high-efficiency OPV cells.

Key words: Rubbing technique, grooved surface, organic photovoltaic cells, bulk heterojunction solar cells.

1. Introduction

OPV (Organic photovoltaic) cells have been fleetly developed in the past years since the solar energy is one of the most abundant sources in the earth and could be regarded as a prevailing technology to convert sunlight into electricity [1]. In particular, it provides relatively inexpensive materials and simple solution processable substitutes to inorganic-based photovoltaic devices [2]. In addition, the advantages of using solar cell devices over organic systems are mechanical flexibility, light weight, and can be using roll-to-roll manufacturing

method at low temperatures. One of the most representative polymer solar cells is the device based on a blend of P3HT [poly (3-hexylthiophene)] as an electron donor and a soluble C₆₀ derivative, PCBM (6,6-phenyl-C61-butyric acid methyl ester) as an electron acceptor. Although the PCE (power conversion efficiency) of the conventional BHJ (bulk-heterojunction) solar cell architecture consisting of P3HT:PCBM blends has reached 4%~6% by a variety of processes [3-5], its performance is still restrained by a relatively poor carrier transfer property, which has also impeded the path toward commercialization. Many studies have demonstrated that appropriate conjugated conducting polymers are attractive alternatives for applications in organic

Corresponding authors: Chih-Yu Chao and Leeyih Wang, professor, research fields: liquid crystals, structure biology and solid state lighting. E-mail: cychao@ntu.edu.tw.

**Patterning of Poly(3,4-Ethylenedioxythiophene):
Poly(Styrenesulfonate) Films via the Rubbing Method in Organic Photovoltaic Cells**

electronic devices in order to obtain a high-efficiency performance [6, 7]. Accordingly, one of the commonly used semiconductive conjugated polymers is poly (3,4-ethylenedioxythiophene):poly (styrenesulfonate) (PEDOT:PSS) which is favorably available as an aqueous dispersion and often utilized as hole injection layer in polymer electronic devices. PEDOT:PSS also has many functions in electronic devices to enhance the electrode performance by adjusting the work function of an electrode [8, 9], modifying the defects on ITO surface and for implication as a flexible anode [10]. Recently, some research groups have investigated film morphology and electrical properties of PEDOT:PSS by several techniques such as conductive atomic force microscopy (C-AFM) [11], micromolding in capillaries (MIMIC) [12], and nanoimprinting (soft-embossing) method [13]. Although the aforementioned techniques can produce micro/nano scale grating structures of the polymer surfaces, some of these techniques are adverse in some ways. For example, in C-AFM case, the conducting probe demands rather a long time to texture the surface features and causes decrease of local film conductivity owing to mass transport of PSS-rich regions to the surface under applied bias. The effective area is also limited by the inherent trait of tip size. As for the MIMIC process, it preferably creates edge thickening arising from a meniscus at the interface between the PDMS mold wall and the polymer solution. The very slow filling rate of small capillaries may hinder the possibility of MIMIC in many types of fabrication system. In addition, the nanoimprinting method requires a sophisticated and elaborate mold to duplicate and transfer grating patterns during direct contact with the polymer surface. Furthermore, the heating procedure results in unnecessary or additional annealing effect on the photoactive layer in organic electronic devices. In most conditions, however, conducting polymers have to be modified to work with these techniques.

In the present work, we demonstrate the

implementation of the rubbing method in the fabrication of an organic-based bulk heterojunction solar cell. The rubbing procedure is the most widely used industrial technique for rapid, simple and inexpensive formation of alignment polymer film over large areas in LCDs (liquid crystal displays) [14]. As a result of previous reports and other papers [15, 16], it is well known that the director of nematic LC (liquid crystal) tends to assume an orientation parallel to the direction in which an adjacent solid surface has previously been rubbed. A crucial concept is that LC molecules could be uniformly oriented by the grooves (wavy surface) of the organic material layer which is caused in the rubbing action. In these studies, these grooves had periods in the range of micrometers to hundreds of nanometers, with relief depths between a few tens and a few hundreds of nanometers. The surface properties of different surface roughness induced by rubbing method were related to polymer structural, morphological and optical properties. Therefore, the employment of periodic structures as an efficient light-trapping plot was investigated for high performance OPV (organic photovoltaic) cells based on P3HT and PCBM bulk heterojunction. The nanoscale grooves of PEDOT:PSS layer were achieved by a lithography free method, so called rubbing process. With this configuration, the periodic grooves increase light absorption in consequence of scattering light occurring within the hole carrier transporting interface between the rubbed PEDOT:PSS and the photoactive layer. Moreover, the morphology of the rubbed PEDOT:PSS surface facilitates the hole carrier collection rate owing to the increased surface area of the interfaces. Most important of all, there are no further modification or treatment on the PEDOT:PSS solution, for example dilution and extra additives. The PCE of polymer solar cells inserted with a grooved PEDOT:PSS layer was enhanced by a simple and fast rubbing treatment. The related measurements and results of this rubbed buffer layer in BHJ solar cell devices suggest the feasibility of this renowned

rubbing method can be applicable to large scale fabrication of polymer based solar cells.

2. Experiments

Here we demonstrate an unprecedented approach, namely rubbing method, of using wavelength scale structure to increase the incident light absorption in organic photovoltaic cells. Fig. 1 shows the flow chart of the fabrication process. First, the ITO glass substrate was cleaned with detergent, acetone and isopropyl alcohol in an ultrasonic bath, before being dried under nitrogen flow. The PEDOT:PSS (Clevios P VP AI4083, H.C. Starck) was spin-coated (40 nm) on the ITO surface, followed by heating at 140 °C for 10 min. In general, the rubbing process is performed by contacting and moving a rotating cylinder (covered with a rubbing cloth) over a polymer-coated substrate at a constant velocity which is shown in Fig. 1a. The grooves (grating-like features) were produced on the PEDOT:PSS surface by the rubbing procedure. The rubbing treatment which is a physical activity was done using a machine whose drum was wrapped with a velvet cloth. Rubbing the surface scribes small grooves (or threads) on the PEDOT:PSS surface as presented in Fig. 1b. The grooves produced during rubbing process are grating-like structure with a periodicity of 500 nm. All the rubbing steps were performed in ambient conditions. The rubbed or un-rubbed PEDOT:PSS-coated substrates were prepared for the next step of active layer coating. Regioregular P3HT was prepared using the Grignard Metathesis approach [17], providing regiocontrol in each coupling step in the polymeric reaction. The regioregularity was characterized by ¹H NMR to be greater than 96%. The mixtures of P3HT (15 mg·mL⁻¹) and PCBM (Nano-C, 12 mg·mL⁻¹) were dissolved in 1 mL of chlorobenzene. Meanwhile, those PEDOT:PSS-coated substrates were transferred into a nitrogen-filled glove box. Then the P3HT:PCBM blend was spin-coated on top of the PEDOT:PSS pre-coated ITO substrate (15 Ω·□⁻¹), and a P3HT:PCBM active layer of about 130 nm was

formed. Subsequently, metallic cathodes of Ca (20 nm) and Al (100 nm) were deposited on top of the active layer by thermal evaporation at a pressure of approximately 10⁻⁶ Torr. The complete solar cell device is exhibited in Fig. 1c. The device area was 0.06 cm² which was defined through a shadow mask allowing the realization of four cells onto the same substrate. Devices to be annealed were placed on a digitally controlled hot plate at 150 °C for 10 min under N₂ atmosphere after the cathode was evaporated.

To study the performances of solar cells with or without rubbed PEDOT:PSS layer, current density-voltage (J-V) characteristics were measured using a programmable Keithley mode 2400 instrument. The solar simulator (Oriel 91160) consists of an Oriel xenon arc lamp with an AM 1.5G solar filter and the 100 mW·cm⁻² intensity was calibrated with a mono-Si reference cell with a KG5 filter (PV Measurements, Inc.), which was calibrated by National Renewable Energy Laboratory (NREL), according to the procedure

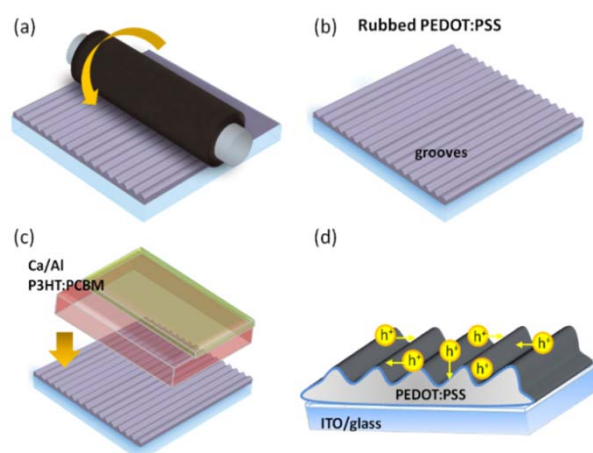


Fig. 1 Schematic representation of the flow chart of the rubbing process applied in the formation of nanoscale grooves on the PEDOT:PSS surface. (a) The PEDOT:PSS-coated film is rubbed by a rotating cylinder which is covered with velvet cloth. (b) The rubbed grooves produced during rubbing process is a wavy-like structure with a periodicity of 500 nm and around 10 nm deep. (c) The polymer solar cell device structure consists of ITO/rubbed PEDOT:PSS/P3HT:PCBM/Ca/Al. (d) Schematic diagram of a larger interface area made by the rubbing process and continuous hole carrier transporting pathways to the ITO electrode.

described elsewhere [18]. The mismatch factor was not considered here. The morphology of the rubbed PEDOT:PSS surface and the thickness of each layer were investigated using the atomic force microscope (AFM). The UV-vis absorption and photoluminescence spectra of the active layer were visualized with the aid of a UV-vis spectrometer (JASCO V-670) and Fluorolog Tau 3 (Jobin Yvon), respectively. The reflectance spectra of the active film were obtained by using a UV-vis-NIR spectrometer (JASCO ILN-725) with an integrating sphere. The IPCE (incident-photon-to-current conversion efficiency) spectra were recorded under illumination by a 450 W xenon lamp with a monochromator (TRIAX 180, JOBIN YVON), and the light intensity was calibrated using an OPHIR 2A-SH power meter. All reflectance, UV-vis, and PL samples were prepared by spin-coating the blend solution of P3HT and PCBM on the PEDOT:PSS/ITO substrates which include the rubbed and non-rubbed samples. To make hole-only devices, Ca/Al was replaced with higher work function Au as the top contact. A 100 nm thickness of Au layer was thermally evaporated on top of the active layer under a pressure of 4×10^{-6} Torr. In order to have reference measurements for the photovoltaic behavior, we classify these samples into the rubbed and the planar solar cell device, respectively.

3. Results and Discussion

To highlight the scientific and technological challenges for highly efficient organic solar cells, we discuss some parameters strongly depending on the morphology of rubbed PEDOT:PSS layer in organic BHJ solar cells which were compared with equivalent cells made by the conventional processing methods. In most rubbing cases, the polymer film is rubbed with another organic polymer material, also called “cloth” which is composed of the synthetic fibers having a variety of chemical structures. It is the nature of the rub material as well as the surface coating that determines the microscopic structure of the treated surface layer

[19]. Reportedly the action of rubbing produces very high localized heating which results in melting of one of the polymer materials [20]. It means that the material with higher melting temperature causes melting of the material with lower melting point. Since the heating generated in the rubbing process is enough to melt the PEDOT:PSS film ($T_m = 149^\circ\text{C}$) locally [19-21]. In our case, the cloth via rubbing process accounts for the oriented grooves produced in PEDOT:PSS layer. The rubbing treatment leads to the nanoscale-groove structure on the surface of PEDOT:PSS layer. The RS (rubbing strength) is expressed by the following formula [22]:

$$RS = NM(2\pi rn/\nu-1) \quad (1)$$

where, N is the number of the repeated times for the rubbing (usually $N = 1$ in our work), M is the depth of the deformed fibers of the cloth due to the pressed contact (mm), n is the rotation rate of the drum ($1,700/60 \text{ s}^{-1}$), ν is the translating speed of the substrate ($20.0 \text{ mm}\cdot\text{s}^{-1}$), and r is the radius of the drum. The RS is given in mm unit. In this research the calculated RS is about 396 mm ($M \sim 1 \text{ mm}$, $r = 42 \text{ mm}$, $n = 28.3 \text{ Hz}$, and $\nu = 20.0 \text{ mm}\cdot\text{s}^{-1}$).

The AFM images shown in Fig. 2 were captured in tapping mode, revealing the surface relief structure of the planar and the rubbed PEDOT:PSS films. In Fig. 2a the planar PEDOT:PSS layer shows flat surface while the rubbed PEDOT:PSS layer in Fig. 2b demonstrates that the orientation of grooves is uniformly aligned

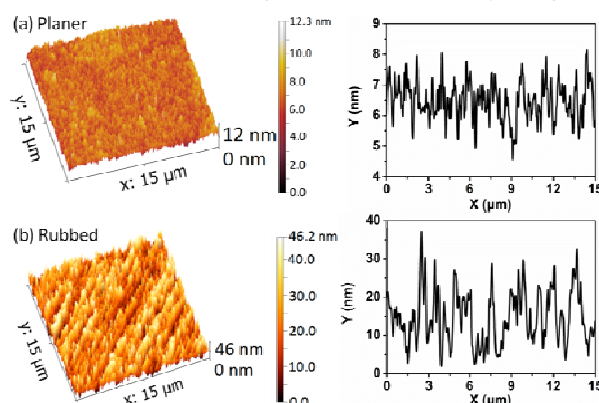


Fig. 2 The surface topography and height variation of (a) planar and (b) grooved PEDOT:PSS films prepared by the rubbing process. (AFM image dimensions: $15 \mu\text{m} \times 15 \mu\text{m}$).

along the rubbing direction. The profile of the rubbed structure shows that the periodicity of the wavy-like grooves is ~ 500 nm, and the depth of the feature is ~ 10 nm. Wavelength scale structures can modify the generation and propagation of light in materials [23]. In addition, small-scale corrugation enables large-area PEDOT:PSS/active layer interfaces, the surface roughness (mean roughness) of PEDOT:PSS layer increases from 0.80 nm to 7.63 nm after rubbing treatment. The interface area of the rubbed sample increases $\sim 1.10\%$ compared with the planar sample. The enhanced interface makes hole carriers transportation extensive as depicted in Fig. 1d. The expected effect of increased surface area is to reduce the distance which newly separated charge carriers will migrate through organic semiconductors before extraction from the device. Such structuring of the buffer layer would potentially increase the light absorbed within the active layer, since the optical path length is increased for light diffracted at angles other than normal to incident. By means of the rubbing process, polymorphism control of organic semiconductor films could greatly affect photovoltaic device performance. In contrast with photolithographic processes, the approach used in this study is a non-destructive and non-complex approach for patterning polymers. Furthermore, the use of rubbing process has several advantages such as a one-step process, feasible duplication and ease of fabrication.

To further characterize the thin film morphologies, we extracted the values of the hole mobility from the dark current density-voltage characteristics of the hole-only devices. We fabricated these devices using a high work-function material, gold (Au), as cathode to block the injection of electrons. The hole mobility was calculated precisely by fitting the dark J-V curves for single carrier devices using SCLC (space charge-limited current) model at low voltages, where the current is given by the equation [24]:

$$J = 9\epsilon_0\epsilon_p\mu V^2(8L)^{-3} \quad (2)$$

where, $\epsilon_0\epsilon_p$ is the permittivity of the polymer, μ is the

carrier mobility, and L is the device thickness. From the dark J-V curves, the obtained hole mobility of the device with the planar PEDOT:PSS layer is $(6.19 \pm 0.13) \times 10^{-5} \text{ cm}^2\cdot\text{V}^{-1}\cdot\text{s}^{-1}$. On the other hand, for the devices treated with rubbed process, the hole mobility increases to $(7.58 \pm 0.37) \times 10^{-5} \text{ cm}^2\cdot\text{V}^{-1}\cdot\text{s}^{-1}$. The increased hole mobility observed upon rubbed PEDOT:PSS layer suggests that the rubbing process benefits to increase the interface area between PEDOT:PSS and the photoactive layer which facilitates hole carrier transportation. Since the electron mobility of PCBM is larger than the hole mobility of conjugated polymer, hole accumulation often occurs in the device and the photocurrent is space-charge limited, leading to a lower fill factor [25]. In our experiments, the hole mobility in the polymer increases by almost 22% so that the electron/hole transport becomes fairly balanced. As a result, the relatively high hole mobility of the rubbed PEDOT:PSS sample increases as a consequence of efficient hole collection via increased contact area, leading to a better device efficiency.

The photovoltaic performance of the P3HT:PCBM based organic photovoltaic cells inserted with planar and rubbed PEDOT:PSS films, under the AM 1.5 G illumination at an incident intensity of $100 \text{ mW}\cdot\text{cm}^{-2}$ is shown in Fig. 3. The planar device exhibits an open-circuit voltage (V_{oc}) of 0.59 V, a short-circuit

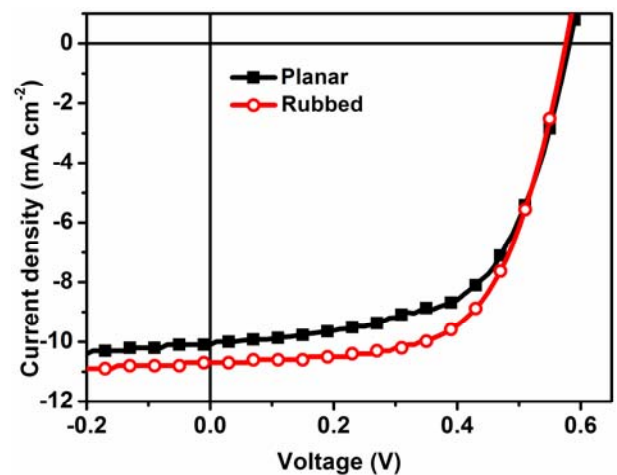


Fig. 3 J-V characteristics (AM 1.5 G, $100 \text{ mW}\cdot\text{cm}^{-2}$) of P3HT:PCBM based solar cells inserted with the planar and the rubbed PEDOT:PSS films.

**Patterning of Poly(3,4-Ethylenedioxythiophene):
Poly(Styrenesulfonate) Films via the Rubbing Method in Organic Photovoltaic Cells**

current density (J_{sc}) of $10.05 \pm 0.08 \text{ mA}\cdot\text{cm}^{-2}$, a fill factor (F.F.) of $58.7\% \pm 0.4\%$, and a power conversion efficiency (PCE) of $3.45\% \pm 0.05\%$. As expected, the effect of rubbing treatment on PEDOT:PSS surface, we have achieved improved solar cell device performance with an increased J_{sc} of $10.70 \pm 0.07 \text{ mA}\cdot\text{cm}^{-2}$, a raised F.F. of $61.6\% \pm 0.1\%$ and an enhanced PCE of $3.82 \pm 0.03\%$. To determine the effect on the film internal resistance caused by grating morphology, R_s (device series resistances) and R_{sh} (shunt resistances) were derived from the slopes of the J-V curves. The R_s of the rubbed device is reduced by rubbing method (to values as low as $8.44 \text{ }\Omega\cdot\text{cm}^2$), which is consistent with the increased J_{sc} . Also, the rubbed device shows an increased R_{sh} ($\sim 0.55 \text{ k}\Omega\cdot\text{cm}^2$) which corresponds to less chance of charge recombination. Previous work has demonstrated that pentacene preferentially grows on an inclined plane (the hillside of a grain boundary) which was used to induce the bulk phase forming in the early stage of pentacene film growth [26, 27]. Herein, we speculate that the rubbed buffer layer is able to influence the formation of the P3HT bulk phase at small thickness ($< 10 \text{ nm}$) on nanoscale undulated PEDOT:PSS surface and align the P3HT polymer chains. The detailed organic photovoltaic performance parameters of the P3HT:PCBM based solar cells with/without the aid of rubbing process are summarized in Table 1.

Photocurrent generation is mainly governed by three major factors: they are the number of absorbed photons; the numbers of carriers generated by the charge separation of excitons at the donor and acceptor interface and the charge-collection efficiency [28]. In order to characterize the optical performance of planar and rubbed PEDOT:PSS samples, the absorption spectra of P3HT:PCBM films on each sample were examined. Fig. 4 shows the absorption spectra of

P3HT:PCBM films on the planar and rubbed PEDOT:PSS layer. There are three vibronic absorption shoulders at 525, 555 and 600 nm, respectively, in the visible region for the P3HT:PCBM blend films, which can be ascribed to the absorption of P3HT. The peak at 525 nm is the absorption of P3HT main chain, and the other two peaks in the longer wavelength are due to the interchain interactions in the ordered P3HT crystalline regions in the films [29]. Comparing two samples with the same active layer thickness, an obvious enhancement in absorption around 525 and 555 nm is observed in the sample with the rubbed PEDOT:PSS layer. The features of rubbed PEDOT:PSS layer can be used as subwavelength scattering elements to couple and trap freely propagating light into an active layer, by diffracting the light into the photon absorber [30]. The scattered light has longer pathways in the active layer and thus increases the possibility of photon absorption. This method could be regarded as a promising approach to improve light absorption without increasing photoactive-layer thickness. Moreover, the rubbed PEDOT:PSS surface shows higher reflectance relative to the planar sample (Fig. 5), which leads to more photons reflected from metal cathode reflected back to the active layer, results in more possibility of photon absorption. Irregularities in grooves will assist the rubbed device to make a broadband collection of photons in order to increase the photocurrent.

The photoluminescence spectra of devices with different PEDOT:PSS films were measured at an excitation wavelength of 550 nm and shown in Fig. 6. The photoluminescence intensity of the P3HT:PCBM film on the planar PEDOT:PSS layer exceeds that of the one on the rubbed surface although the latter has higher absorbance at the excitation wavelength. This finding supports the presence of the grooving structure can greatly increase the interfacial area between the

Table 1 The performance parameters of P3HT:PCBM based solar cells with/without the aid of rubbing process are summarized.

	V_{oc} (V)	J_{sc} ($\text{mA}\cdot\text{cm}^{-2}$)	F.F. (%)	PCE (%)	R_s ($\Omega\cdot\text{cm}^2$)	R_{sh} ($\text{k}\Omega\cdot\text{cm}^2$)
Planar	0.59	10.05	58.7	3.45	9.06	0.51
Rubbed	0.58	10.70	61.6	3.82	8.44	0.55

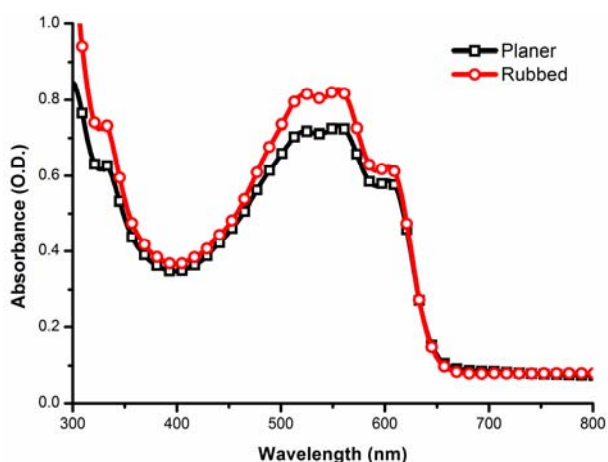


Fig. 4 UV-vis absorption spectra of the active films (P3HT:PCBM = 1:0.8) deposited on the planar and the rubbed PEDOT:PSS layers.

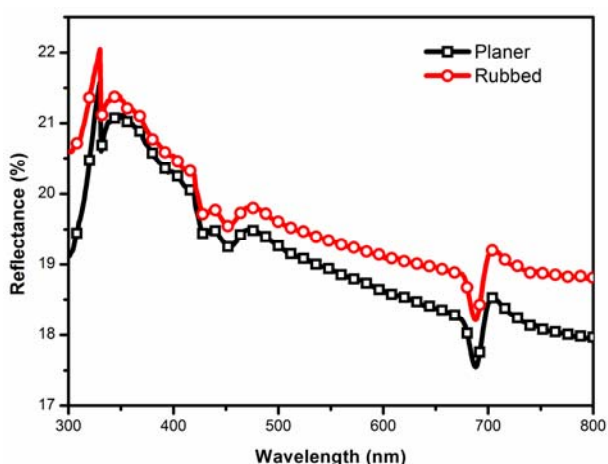


Fig. 5 Reflectance spectra of the planar and the rubbed PEDOT:PSS layers on glass substrates.

blend materials and the buffer layer and the efficiency of photoinduced carrier transfer. Besides, it has been shown that the amount of PCBM in active layer is richer than P3HT near the surface of PEDOT:PSS layer, which increases the possibility of electron/hole recombination when hole carriers transport toward buffer layer [31]. Therefore, the undulated surface of PEDOT:PSS layer, which can be viewed as a protrusion sticking out into the active layer, could further enhanced the interface between PEDOT:PSS and the P3HT-rich part in the active layer as Fig. 6b illustrated. As a result, controlling the surface morphology can facilitate extraction of holes as it will in some regions shorten the distance they have to travel

to the electrode. The rubbing method induced performance improvement is attributed to the increased number of absorbed photons and promoting carrier transport behavior.

Consequently, as shown in Fig. 7, the device with the rubbed layer demonstrates higher IPCE throughout the visible range compared with the device without the rubbed layer. Because the integration of the product of the IPCE with the AM 1.5G solar spectrum is equal to J_{sc} , the higher J_{sc} (Fig. 3) of the device with rubbed layer is consistent with the higher IPCE values. All IPCE curves closely follow the absorption spectra of the P3HT:PCBM blend and maximum efficiency wavelength of the IPCE located at around 525 nm. Enhancement of PCE inherently coupled with enhanced

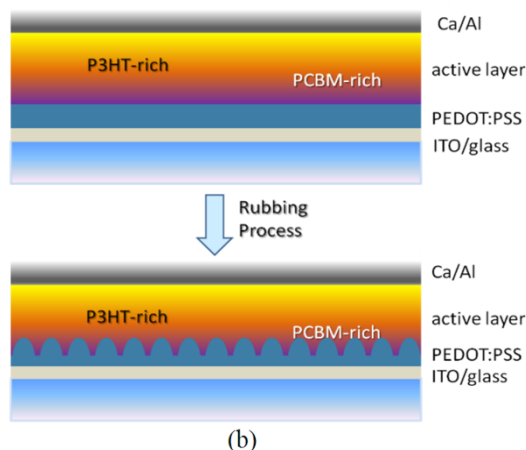
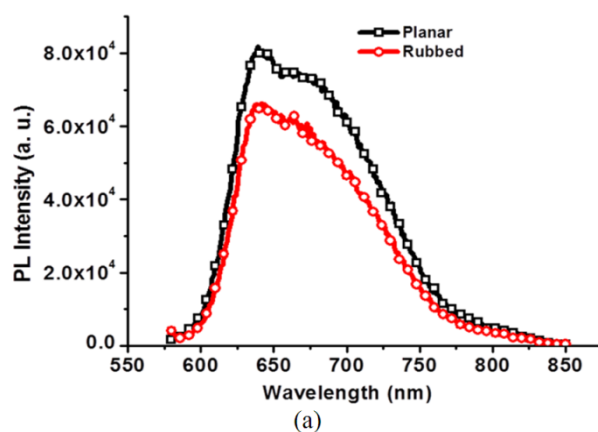


Fig. 6 (a) Photoluminescence spectra of the active films (P3HT:PCBM = 1:0.8) deposited on the planar and the rubbed PEDOT:PSS layers and (b) schematic diagram of the interface enhancement between PEDOT:PSS and the P3HT-rich part in the active layer.

**Patterning of Poly(3,4-Ethylenedioxythiophene):
Poly(Styrenesulfonate) Films via the Rubbing Method in Organic Photovoltaic Cells**

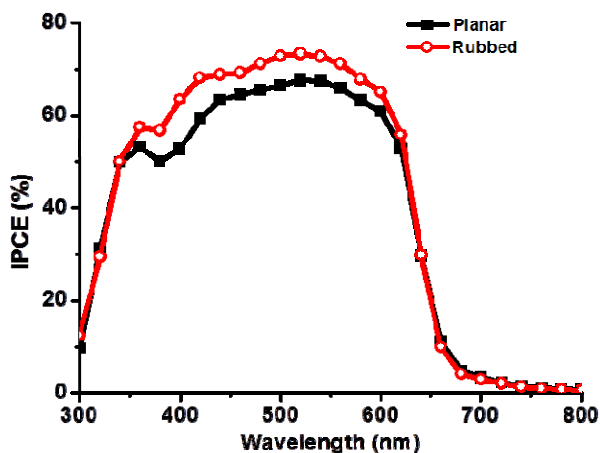


Fig. 7 IPCE spectra of P3HT:PCBM based solar cells inserted with the planar and the rubbed PEDOT:PSS films.

photon absorption for increased exciton generation and subsequent exciton dissociation efficiency gains to form free charge carriers. At maximum peak position the enhancement of IPCE is around 10%. Here, most of the increase in the cell efficiency is from the increased J_{sc} through the application of periodic structures rather than V_{oc} . It means that rubbed grooves induce more photogenerated charge carriers by stronger absorption of an active layer, resulting from the increase of optical path length and light trapping. IPCE and PCE of OPV cells with grooved buffer layers increase primarily due to enhanced J_{sc} , indicating the grooves created by the rubbing method cause further photon absorption in active layers and better hole transportation (charge carrier mobility) within the interface between PEDOT:PSS and the active layer. In addition, the size effect of grooves could be one of the factors for such results. Further studies by the authors are under progress and will be reported in due course.

4. Conclusions

We envisage that the grooved structure could readily be mass produced by the rubbing method, a technique that is very mature and successfully used for the manufacture of LCDs, has been unprecedentedly demonstrated for organic photovoltaic cells. In our work, the obtained PCE in the presence of a rubbed PEDOT:PSS layer is 3.82%, which is higher than the

corresponding PCE 3.45% of the planar device. Moreover, the hole carrier mobility, optical absorbance, and excitons dissociation rate have been improved due to the resultant grooved morphology on the surface of PEDOT:PSS layer. This synergistic performance enhancement is believed to originate from the oriented interfaces that facilitate charge transport, moderate ordering of bulk heterojunction materials near the interfaces, and some light scattering to the photoactive layer from the nanoscale grooved surface. As this simple rubbing technique is inexpensive and suitable for roll-to-roll manufacturing over large areas, it may contribute to the goal of efficient solar energy conversion using organic polymers and molecules. From this standpoint, the rubbing technique is a potential technology for large scale fabrication of polymer based solar cells.

Acknowledgments

This work was supported by the National Science Council and Ministry of Education of the Republic of China. The authors would like to thank Dr. Chin-Wei Liang for his assistance and helpful discussions.

References

- [1] C.J. Brabec, N.S. Sariciftci, J.C. Hummelen, Plastic solar cells, *Adv. Funct. Mater.* 11 (2001) 15-26.
- [2] G. Li, V. Shrotriya, J. Huang, Y. Yao, T. Moriarty, K. Emery, et al., High-efficiency solution processable polymer photovoltaic cells by self-organization of polymer blends, *Nat. Mater.* 4 (2005) 864-868.
- [3] W.L. Ma, C.Y. Yang, X. Gong, K.H. Lee, A.J. Heeger, Thermally stable, efficient polymer solar cells with nanoscale control of the interpenetrating network morphology, *Adv. Funct. Mater.* 15 (2005) 1617-1622.
- [4] Y. Kim, S. Cook, S.M. Tuladhar, S.A. Choulis, J. Nelson, J.R. Durrant, et al., A strong regioregularity effect in self-organizing conjugated polymer films and high-efficiency polythiophene: Fullerene solar cells, *Nat. Mater.* 5 (2006) 197-203.
- [5] G. Zhao, Y. He, Y. Li, 6.5% efficiency of polymer solar cells based on poly(3-hexylthiophene) and indene-C60 bisadduct by device optimization, *Adv. Mater.* 22 (2010) 4355-4358.
- [6] B. Crone, A. Dodabalapur, Y.Y. Lin, R.W. Filas, Z. Bao, A. LaDuca, et al., Large-scale complementary integrated

- circuits based on organic transistors, *Nature* 403 (2000) 521-523.
- [7] L.B. Groenendaal, F. Jonas, D. Freitag, H. Pielartzik, J.R. Reynolds, Poly(3,4-ethylenedioxythiophene) and its derivatives: Past, present, and future, *Adv. Mater.* 12 (2000) 481-494.
- [8] T.M. Brown, J.S. Kim, R.H. Friend, F. Cacialli, R. Daik, W.J. Feast, Built-in field electroabsorption spectroscopy of polymer light-emitting diodes incorporating a doped poly(3,4-ethylene dioxythiophene) hole injection layer, *Appl. Phys. Lett.* 75 (12) (1999) 1679-1681.
- [9] V. Shrotriya, G. Li, Y. Yao, C.W. Chu, Y. Yang, Transition metal oxides as the buffer layer for polymer photovoltaic cells, *Appl. Phys. Lett.* 88 (2006) 073508-073510.
- [10] D. Li, L.J. Guo, Micron-scale organic thin film transistors with conducting polymer electrodes patterned by polymer inking and stamping, *Appl. Phys. Lett.* 88 (2006) 063513-063515.
- [11] X.D. Dang, M. Dante, T.Q. Nguyen, Morphology and conductivity modification of poly(3,4-ethylenedioxythiophene):poly(styrene sulfonate) films induced by conductive atomic force microscopy measurements, *Appl. Phys. Lett.* 93 (2008) 241911-241913.
- [12] F. Zhang, T. Nyberg, O. Inganäs, Conducting polymer nanowires and nanodots made with soft lithography, *Nano Lett.* 2 (2002) 1373-1377.
- [13] Y. Yang, K. Lee, K. Mielczarek, W. Hu, A. Zakhidov, Nanoimprint of dehydrated PEDOT:PSS for organic photovoltaics, *Nanotechnology* 22 (2011) 485301-485305.
- [14] P.G. de Gennes, J. Prost, *The Physics of Liquid Crystals*, Oxford University Press, New York, 1993, pp. 34-35.
- [15] M. Nishikawa, N. Bessho, T. Natsui, Y. Ohta, N. Yoshida, D.S. Seo, et al., A model of the unidirectional alignment accompanying the pretilt angle of a nematic liquid crystal (NLC), 5CB, oriented on rubbed organic-solvent-soluble polyimide film, *Mol. Cryst. Liq. Cryst.* 275 (1996) 15-25.
- [16] D.S. Seo, O.I. Toshio, H. Matsuda, T.R. Isogami, K.I. Muroi, Y. Yabe, et al., Surface morphology of the rubbed polyimide and polystyrene films and their liquid crystal aligning capability, *Mol. Cryst. Liq. Cryst.* 231 (1993) 95-106.
- [17] R.S. Loewe, S.M. Khersonsky, R.D. McCullough, A simple method to prepare head-to-tail coupled, regioregular poly(3-alkylthiophenes) using grignard metathesis, *Adv. Mater.* 11 (1999) 250-253.
- [18] V. Shrotriya, G. Li, Y. Yao, T. Moriarty, K. Emery, Y. Yang, Accurate measurement and characterization of organic solar cells, *Adv. Funct. Mater.* 16 (2006) 2016-2023.
- [19] J.A. Castellano, Surface anchoring of liquid crystal molecules on various substrate, *Mol. Cryst. Liq. Cryst.* 94 (1983) 33-41.
- [20] A. Adamson, *Physical Chemistry of Surfaces*, John Wiley & Sons, 3rd ed., New York, 1976, p. 246.
- [21] M.D. Irwin, D.A. Roberson, R.I. Olivas, R.B. Wicker, E. MacDonald, Conductive polymer-coated threads as electrical interconnects in e-textiles, *Fiber Polym.* 12 (2011) 904-910.
- [22] D.S. Seo, S. Kobayashi, M. Nishikawa, Study of the pretilt angle for 5CB on rubbed polyimide films containing trifluoromethyl moiety and analysis of the surface atomic concentration of F/C(%) with an electron spectroscopy for chemical analysis, *Appl. Phys. Lett.* 61 (1992) 2392-2394.
- [23] B.J. Matterson, J.M. Lupton, A.F. Safonov, M.G. Salt, W.L. Barnes, I.D. Samuel, Increased efficiency and controlled light output from a microstructured light-emitting diode, *Adv. Mater.* 13 (2001) 123-127.
- [24] V. Shrotriya, Y. Yao, G. Li, Y. Yang, Effect of self-organization in polymer/fullerene bulk heterojunctions on solar cell performance, *Appl. Phys. Lett.* 89 (2006) 063505-063507.
- [25] C. Melzer, E.J. Koop, V.D. Mihailetschi, P.W.M. Blom, Hole transport in poly(phenylene vinylene)/methanofullerene bulk-heterojunction solar cells, *Adv. Funct. Mater.* 14 (2004) 865-870.
- [26] H.L. Cheng, Y.S. Mai, W.Y. Chou, L.R. Chang, X.W. Liang, Thickness-dependent structural evolutions and growth models in relation to carrier transport property in polycrystalline pentacene thin films, *Adv. Funct. Mater.* 17 (2007) 3639-3649.
- [27] M.H. Chang, W.Y. Chou, Y.C. Lee, H.L. Cheng, H.Y. Chung, Polymorphic transformation induced by nanoimprinted technology in pentacene-film early-stage growth, *Appl. Phys. Lett.* 97 (2010) 183301-183303.
- [28] G. Yu, J. Gao, J.C. Hummelen, F. Wudl, A.J. Heeger, Polymer photovoltaic cells: Enhanced efficiency via a network of internal donor-acceptor heterojunctions, *Science* 270 (1995) 1789-1791.
- [29] P.J. Brown, D.S. Thomas, A. Kohler, J.S. Wilson, J.S. Kim, C.M. Ramsdale, et al., Effect of interchain interactions on the absorption and emission of poly(3-hexylthiophene), *Phys. Rev. B* 67 (2003) 064203-064218.
- [30] H.A. Atwater, A. Polman, Plasmonics for improved photovoltaic devices, *Nat. Mater.* 9 (2010) 205-213.
- [31] M. Campoy-Quiles, T. Ferenczi, T. Agostinelli, P.G. Etchegoin, Y. Kim, T.D. Anthopoulos, et al., Morphology evolution via self-organization and lateral and vertical diffusion in polymer: Fullerene solar cell blends, *Nature Mater.* 7 (2008) 158-164.